

CHAPTER - 5

RESULTS & DISCUSSION

5.1 Effect of Ferrite content on the micro hardness profile

Weld survey results along one side of weld centreline as shown in Fig. 5.1 mentions that weld metal deposited by Low Ni (9.5 – 10.5 wt%), Medium Ni (10.5 -11.5 wt%) enhanced nickel electrodes nearly overlaps around 295 VPN, at fusion boundary. This fact is because of presence of fine ferritic-austenitic grain zone produced in the FZ. As shown in Fig. 5.15, 5.16 & 5.18.

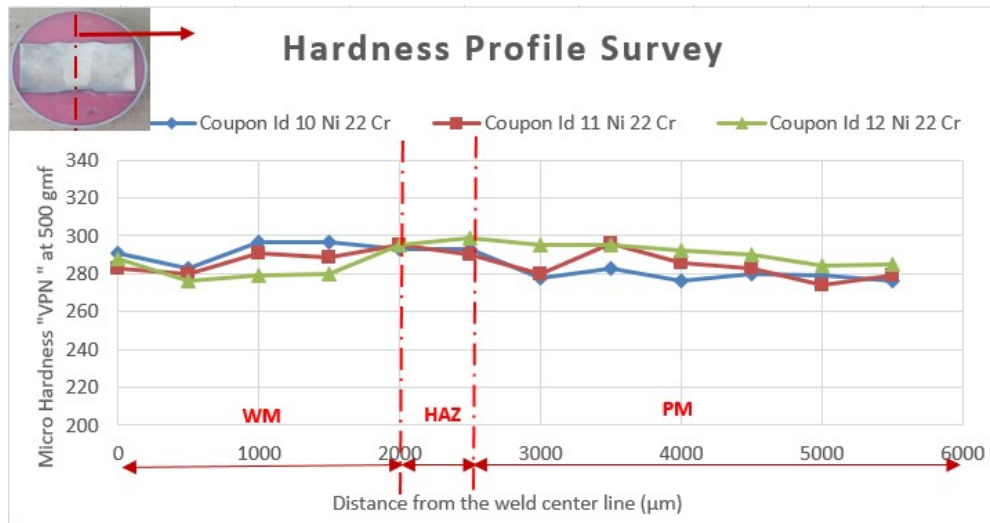


Fig. 5.1 Micro Hardness profile survey measured on 12 locations.

Hardness drops nearly to 276 HV is due to the less existence of Widmanstatten austenite (WA) and intergranular austenite (IGA) in the Fusion Zone. While for Medium nickel added electrodes hardness significantly falls in weld fusion zone which shows more production of austenite due to nickel promoting effect. These facts are supported by the optical metallography as shown in Fig. 5.7 & Fig. 5.8.

5.2 Effect of ferrite content on strength

Table 5.1 All weld metal test results are tabulated as below

| Coupon ID | Ferrite content at T/2 location | | Tensile Strength Mpa | | Yield Strength Mpa (at 0.2% Proof Load) | | % Elongation | | % RA | |
|-------------------------|---------------------------------|-------------------|----------------------|---------|---|-----------------------|--------------|---------|-----------------------|-----------------------|
| | FN | % Ferrite | Sample1 | Sample2 | Sample1 | Sample2 | Sample1 | Sample2 | Sample1 | Sample2 |
| *AWS A5.4 | 30-50 | 30-60 % OR 35-75% | 690 Min | | Spec does not require | Spec does not require | 20 Min | | Spec does not require | Spec does not require |
| # ISO 3581 | 30-50 | 30-60 % OR 35-75% | 550 Min | | 450 Min | 450 Min | 20 Min | | Spec does not require | Spec does not require |
| E2209-16 (9 Ni 22Cr) | 29.0 | 30.12 | 762 | 800 | 660 | 680 | 25.50 | 26.0 | 44.5 | 45.6 |
| 10 Ni 22 Cr (Low Ni) | 31.7 | 31.5 | 853 | 860 | 687 | 684 | 25.7 | 25.3 | 46.5 | 46.3 |
| 11 Ni 22 Cr (Medium Ni) | 28.2 | 27.6 | 858 | 852 | 678 | 683 | 24.6 | 26.0 | 51.0 | 48.7 |
| 12 Ni 22 Cr (High Ni) | 14.0 | 14.4 | 760 | 778 | 588 | 644 | 27.4 | 28.0 | 64.6 | 63.0 |

Note: -

* AWS A5.4 (Specification for Stainless Steel Electrodes for Shielded Metal Arc Welding) E2209-16 Requirements for comparison with the evaluated results

ISO 3581 (Welding consumables -- Covered electrodes for manual metal arc welding of stainless and heat-resisting steels – Classification) 22 9 3 N L or 2209 filler Requirement for comparison with the evaluated results

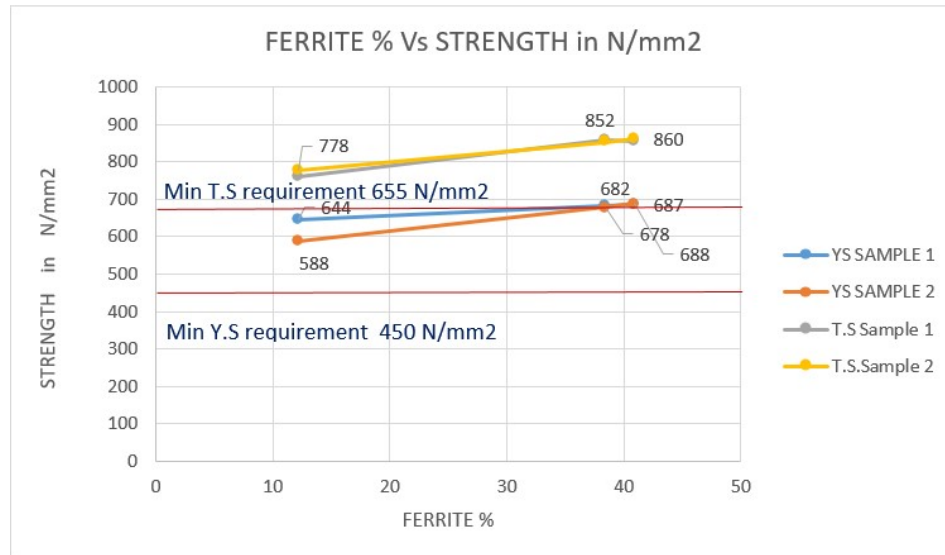


Fig 5.2 Tensile and Yield strength as a function of % Ferrite for 2205

As can be observed from the above result that the tensile and yield strengths are very marginally affected by ferrite content variation from 14% to 30%, or 20 FN to 40 FN, Moreover ASTM A240 standard for 2205 base metal specifies 450 MPa yield strength minimum, and 655 MPa tensile strength minimum. So all-weld metal test results comfortably meet those requirements. It is also noteworthy that AWS A5.4 only specifies tensile strength, not yield strength. Further this is also noteworthy that ISO 3581 requires yield strength for the 22 9 3 N L or 2209 filler metal to be 450 MPa minimum. So all those requirements are exceeded.

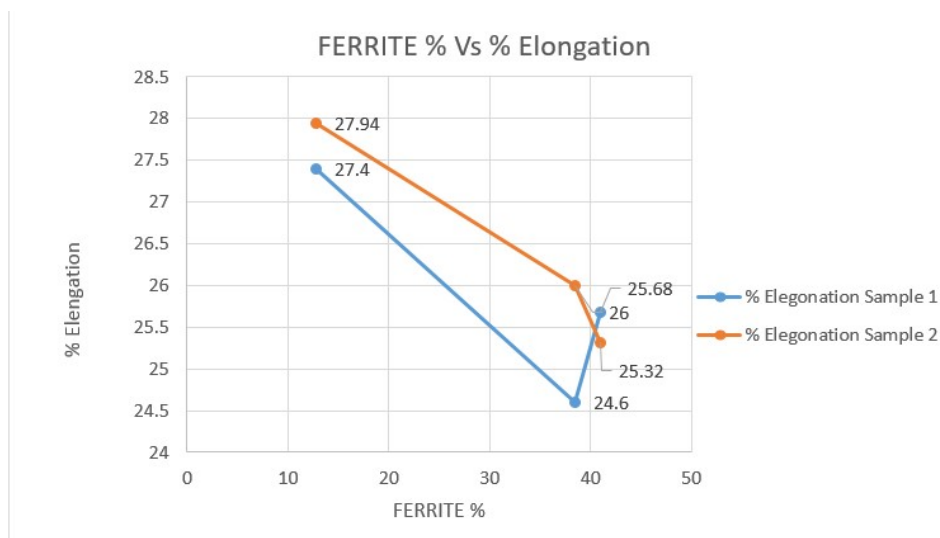


Fig 5.3 Ductility as a function of % Ferrite for 2205

There is a marginal change in the ductile behaviour, between 14-30 % Ferrite, as increase in the ductility beyond 24.5 at nearly 40 % ferrite to 27 % ductility at nearly 15 % Ferrite percentage, can be well expected by effect of nickel as austenite stabilizer, As more production of austenite phase, about 60 to 85 % , in weld deposits result in increase in ductility.

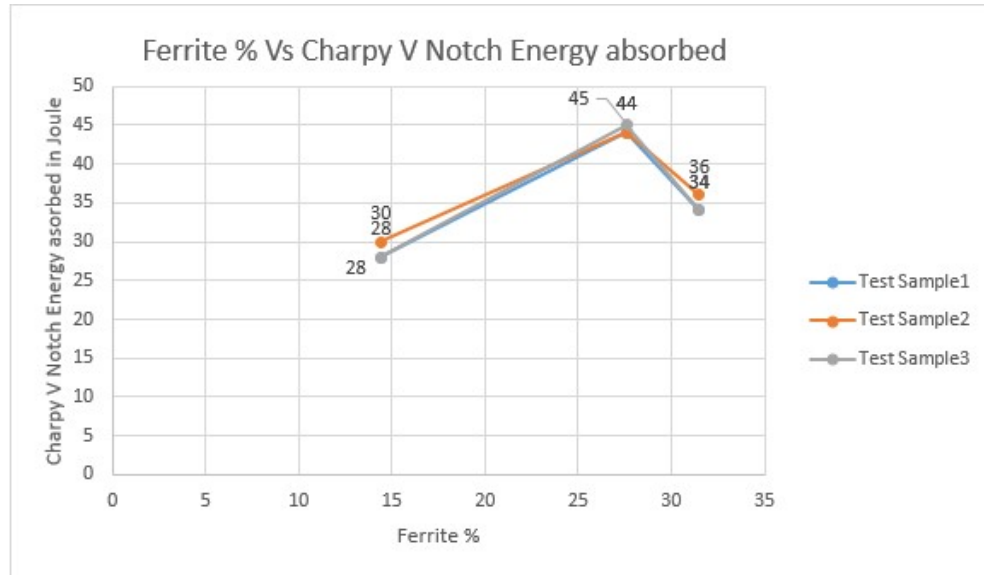


Fig. 5.4 Charpy energy absorbed (Joule) at -40 °C as a function of Ferrite Content for 2205.

Above result indicates that there is a significant decrease in the impact strength values from 46 to 30 Joule, with decrease in Ferrite % from 30 to 14. Normally CVN minimum requirements is 27 Joule at -40°C, which is comfortably exceeded since various welding practice codes may require 27 J, 34 J or 47 J at -40°C. And when the user requires 47 J at -40°C, E2209-15 electrodes are often recommended because E2209-16 electrodes have difficulty meeting the 47J requirement due to the higher side oxygen content of the weld metal with E2209-16.

5.3 Microstructure examinations

Weld test coupon samples were polished and electrochemically etched in 40 gms NaOH in 100 ml distilled Water for 5 Sec as per ASTM A 923-14, Method A which is a quick screening method for identifying intermetallic in the microstructure.

Microstructure shows a typical duplex microstructure of ferrite and austenite. No significant presence of inter-metallic phases and precipitates observed in the microstructure. In Low Ni (9.5-10.5) & Medium Ni (10.5-11.5), An unaffected Structure was observed for all weld test coupon samples, reflecting solidification in the F-mode (essentially 100% ferrite solidification) and formation of austenite only in the solid state, as described by Lippold and Kotecki [1]

The ferrite has been etched without revelation of inter-metallic phase. Interphase boundaries are smooth . Fig 5.5 to 5.14.

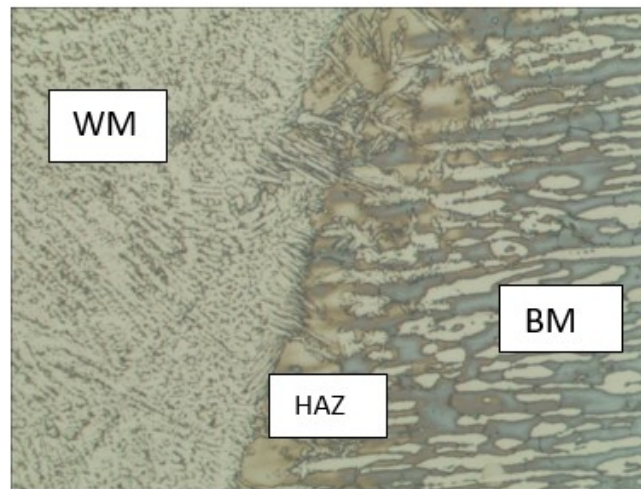


Fig 5.5 FZ / HAZ Interface at 100 X magnification sample 12Ni 22 Cr with 10% NaOH Etched. Ferrite is revealed as dark Phase & Austenite as Light Phase

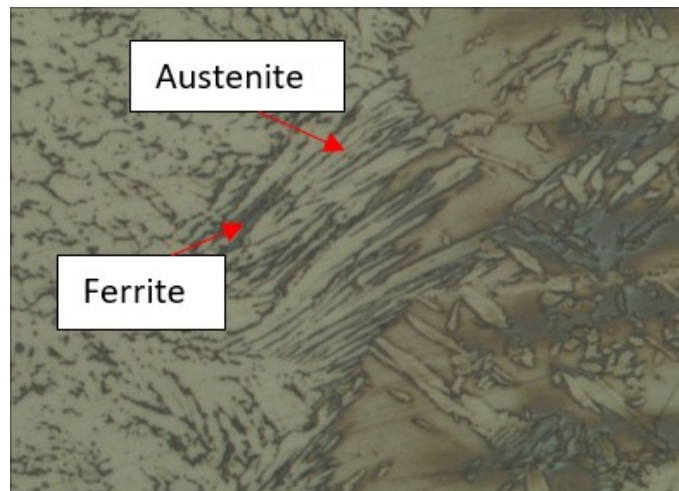


Fig 5.6 FZ / HAZ Interface at 400 X magnification sample 12Ni 22 Cr with 10% NaOH Etched. Ferrite is revealed as dark Phase & Austenite as Light Phase

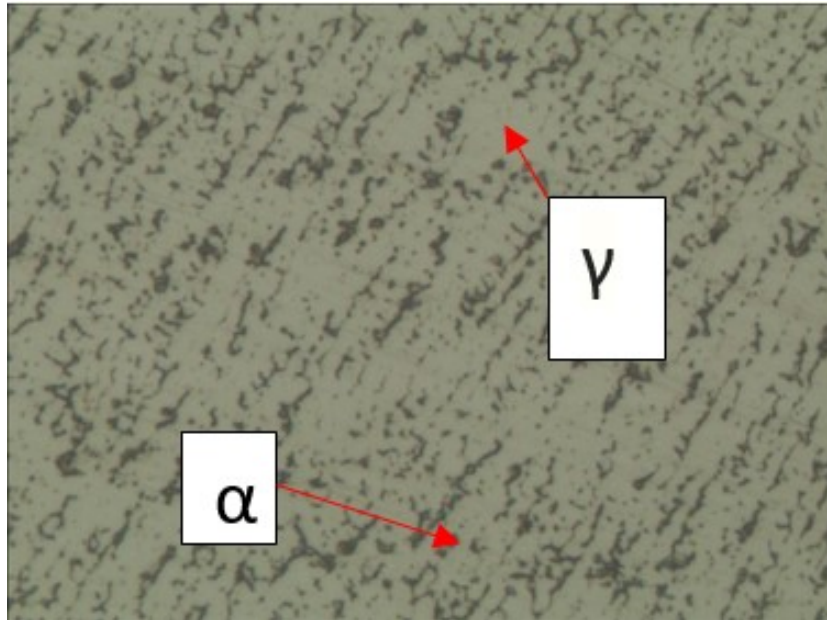


Fig 5.7 FZ Micro at 400 X magnification sample 12Ni 22 Cr with 10% NaOH Etched. Ferrite is revealed as dark Phase & Austenite as Light Phase

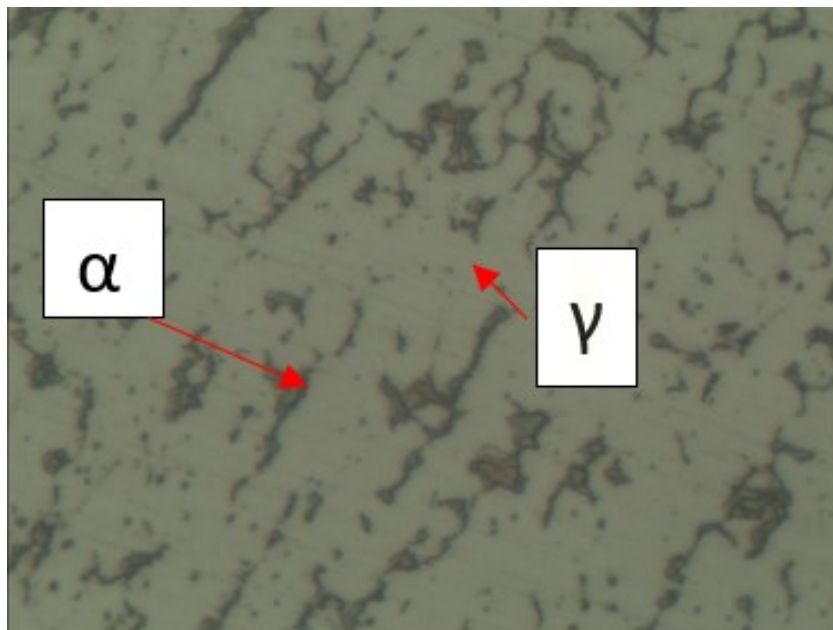


Fig 5.8 FZ Micro at 1000 X magnification sample 12Ni 22 Cr with 10% NaOH Etched. Ferrite is revealed as dark Phase & Austenite as Light Phase

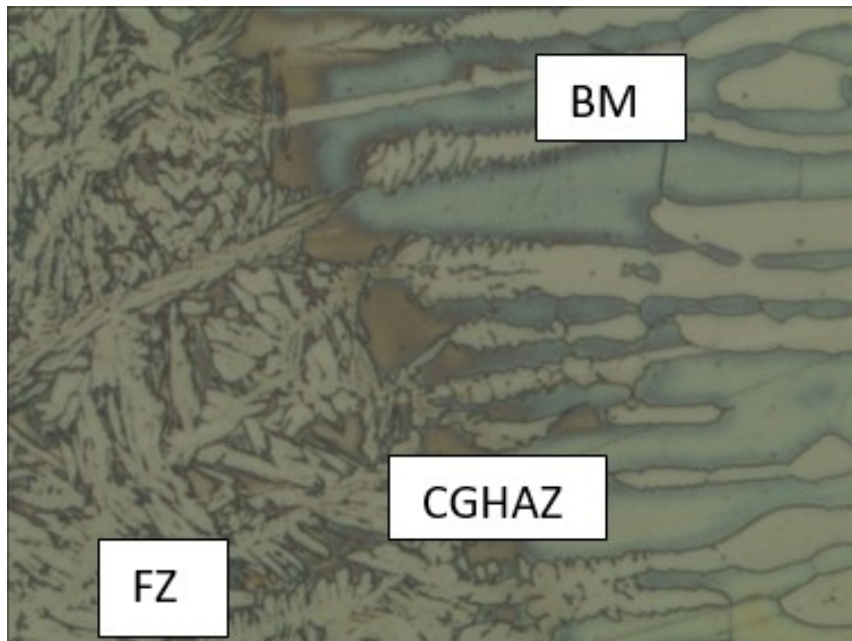


Fig. 5.9 Micro HAZ / FZ Interface at 400 X Magnification revealing coarse grain Heat affected zone (CGHAZ) Sample id 11 Ni 22 Cr

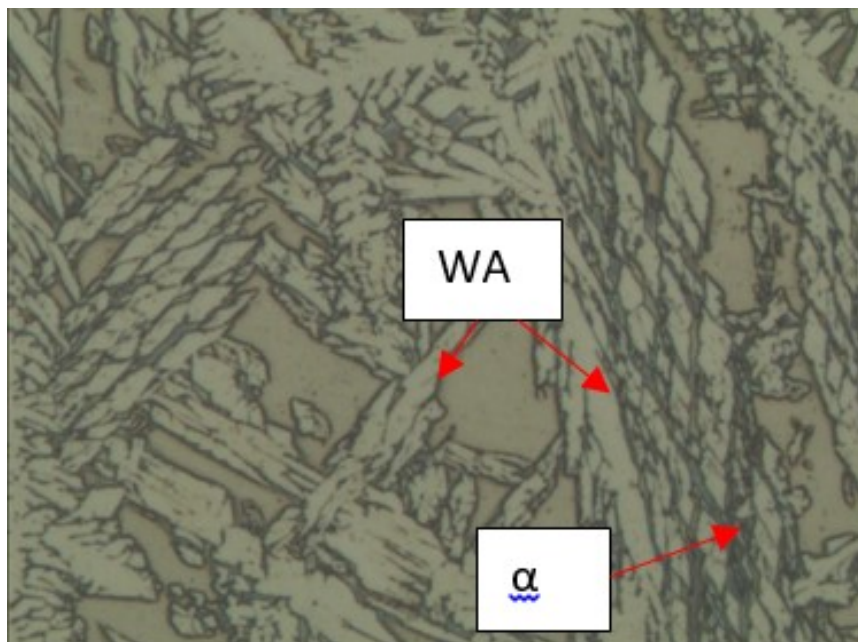


Fig 5.10 Micro of weld at 400 X Mag sample revealing Widmanstatten austenite as light phase and ferrite as dark phase. Sample id 11 Ni 22 Cr

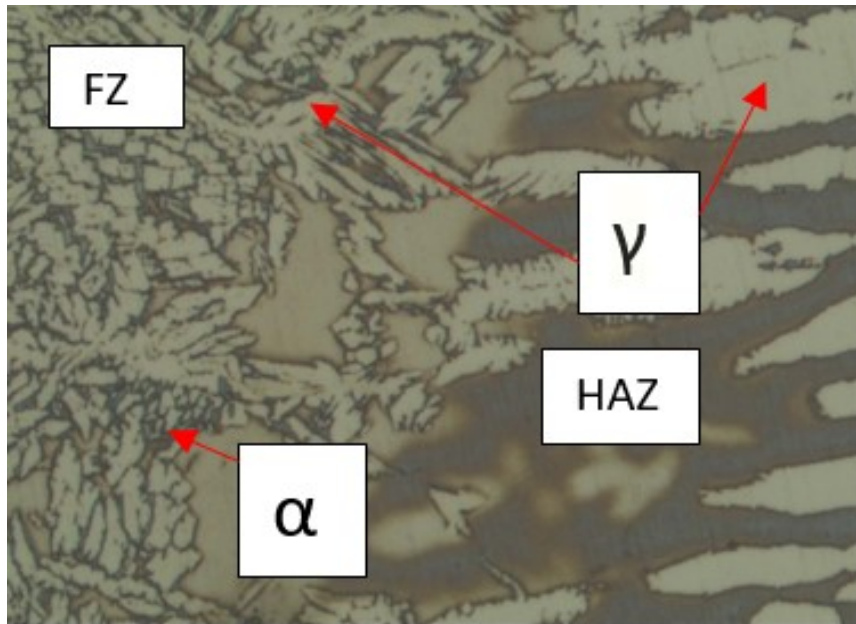


Fig 5.11 FZ / HAZ Interface at 400 X magnification sample 10Ni 22 Cr with 10% NaOH Etched. Ferrite is revealed as dark Phase & Austenite as Light Phase

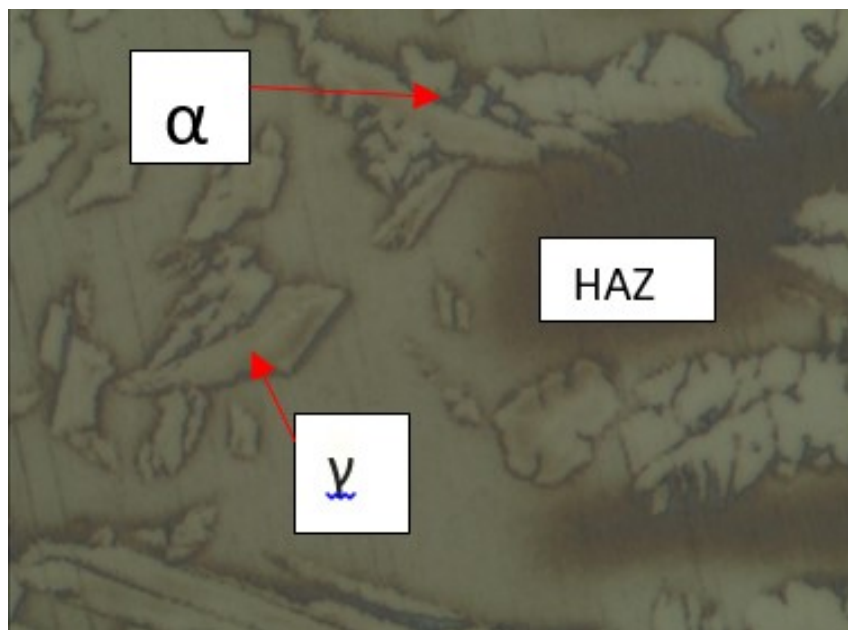


Fig 5.12 FZ / HAZ Interface at 1000 X magnification sample 10Ni 22 Cr with 10% NaOH Etched. Ferrite is revealed as dark Phase & Austenite as Light Phase

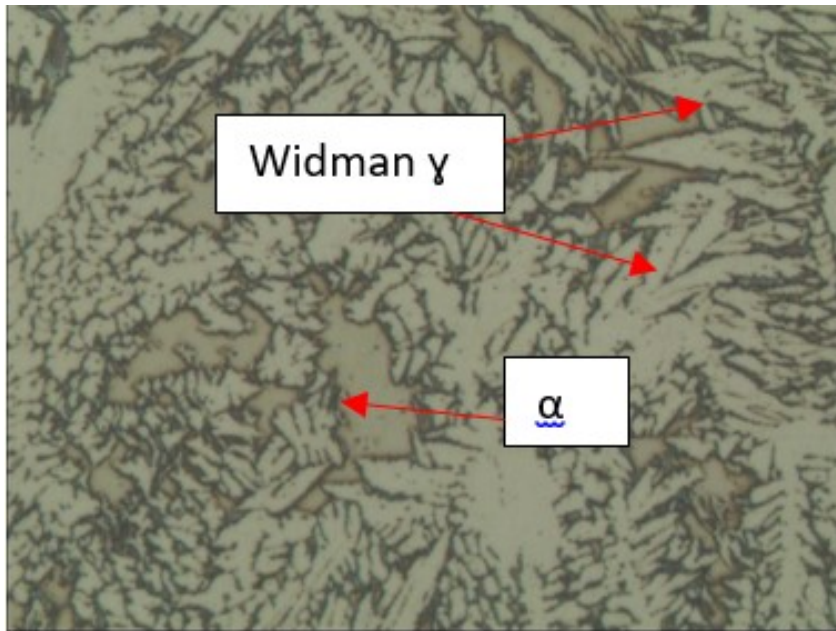


Fig 5.13FZ Micro at 200 x Magnification reveals light phase Widmanstatten Austenite (WA) and Ferrite (Dark Phase) Coupon Id 10Ni 22 Cr

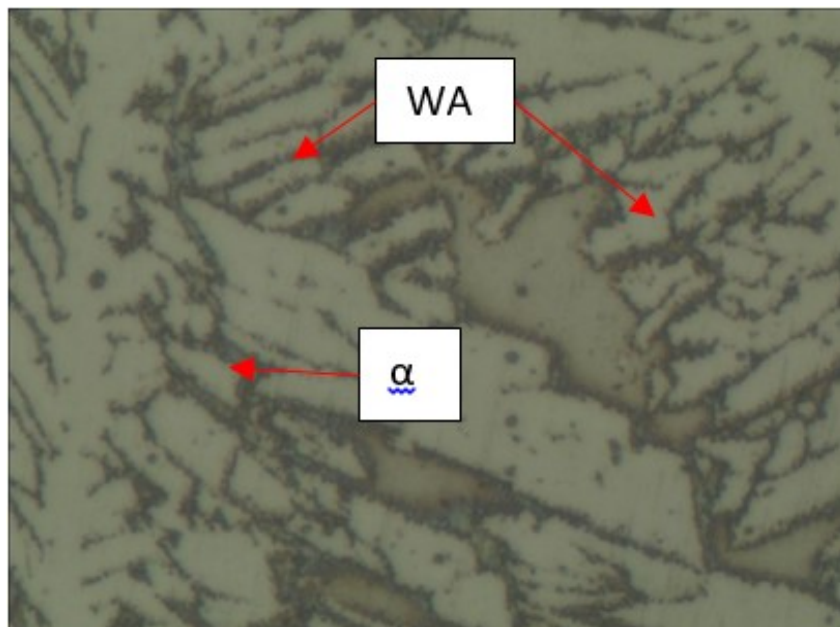


Fig 5.14FZ Micro at 1000 x Magnification clearly reveals light phase Widmanstatten Austenite (WA) and Ferrite (Dark Phase) Coupon Id 10 Ni 22 Cr



Fig. 5.15 sample id 11 Ni 22 Cr Micro at 200 x Magnification,NaOH etched light phase austenite (WA) and ferrite (dark phase)



Fig.5.16 sample id 11 Ni 22 Cr across fusion boundary showing fine grain austenite in fusion zone Weld Micro at 200 X Mag. NaOH etched

The microstructure of the High Nickel 11.5 to 12.5 Ni weld samples are (Fig. 5.6-5.8) considerably different from that of the other two samples Fig (5.8-5.16). There is some plate-like formation of austenite near the fusion boundary (indicating F-mode solidification). However, the remainder of the weld metal near the fusion boundary and at the weld centre exhibits the skeletal ferrite typical of FA-mode solidification

(primary ferrite with austenite appearing during the later stages of solidification), as described by Lippold and Kotecki[1]

5.4 Comparisons of Ferrite Measurement results between ASTM E 562-11: Volume Fraction measurement by systematic Point Count method and Ferriscope ® Instrument

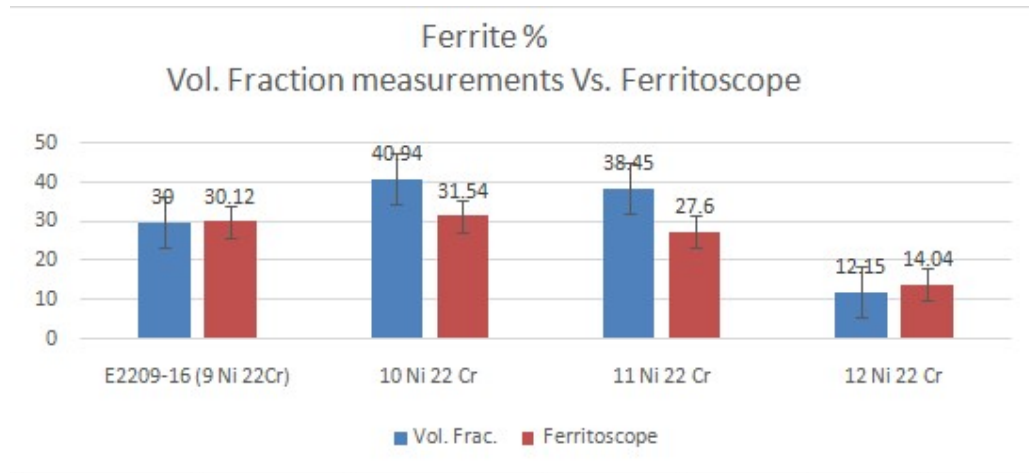
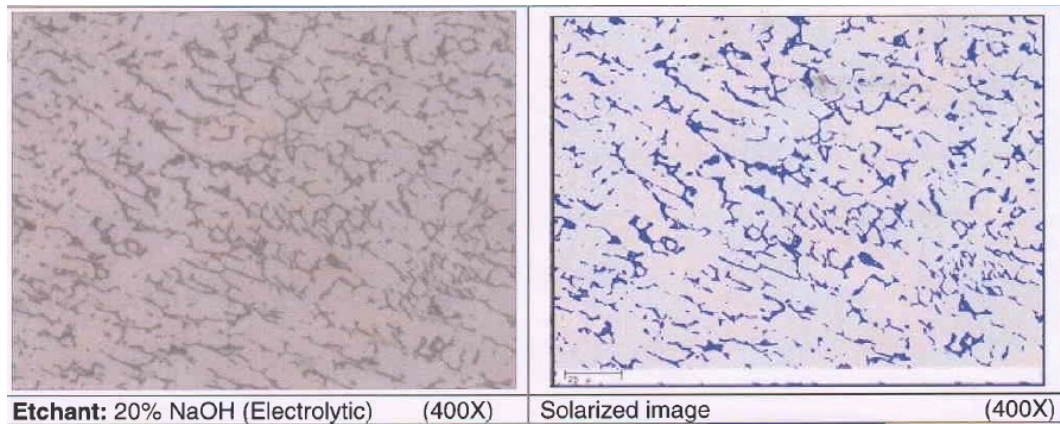


Fig. 5.17 Comparative data of Ferrite measurement by Volume fraction measurement, point count method and Ferriscope instrument.

As can be observed from above graph fig 5.17, ASTM E-562 method relies on the grain morphology, since presence of skeletal ferrite in austenite matrix resulting in High Nickel weld deposits. As nickel being austenite promoter, in 12 Ni 22 Cr sample, more complex grained structure making it difficult to carry out analysis by placement of the points on respective ferritic-austenitic grains, to add in that, the discrete and discontinuous type ferritic and austenitic grains puts limitations on the “statistical analysis” used by the software program. Alternatively volume fraction measurement by using colour distinctions on micro structure some times over reads the ferrite % so instead of ASTM E 562 method , Image Analysis software was used. Fig. 5.18 image analysis software processed micrograph of 10 Ni 22 Cr weld coupon below.



**Fig. 5.18 Fine grain weld metal zone microstructure of 12 Ni 22 Cr weld coupon.
Dark phase is ferrite and light phase is austenite.**

On the contrary, for the clearly distinct ferritic-austenitic grain morphology, i.e. which enables the placement of the points on the ferrite and austenite grains (as shown in fig 5.19), yellow points on lightly etched austenite grains and red points on dark etched ferrite grains) for weld sample 10 Ni 22 Cr shows less deviations of 7 % , while 11 Ni 22 Cr shows 12 % deviation difference in percentage ferrite reading between the two methods, volume fraction method and Feritscope instrument respectively in Fig 5.17. This metallographic method of ferrite measurement relies on many critical factors such as sample preparations quality, magnification and processing of micro image, identification of grains, placement of points on the distinct grains and more importantly users expertise to process and interpret the microstructure.

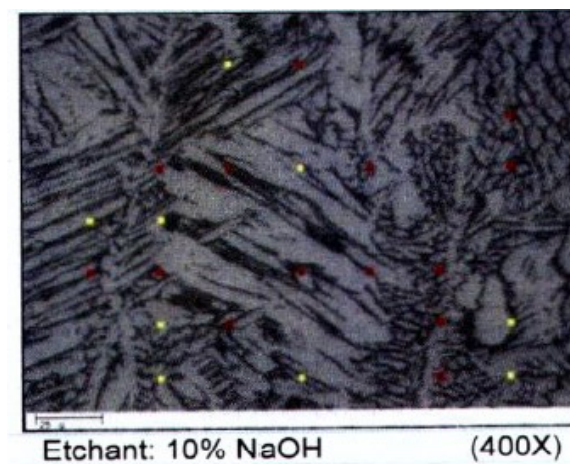


Fig. 5.19 Photomicrograph of 10 Ni 22 Cr Weld coupon 10 % NaOH etched at 400 X magnification reveals dark phase as ferrite and light phase as austenite.

5.5 Comparisons of Ferrite Measurement results between Top surface of Weld deposits and Cross Section of Weld.

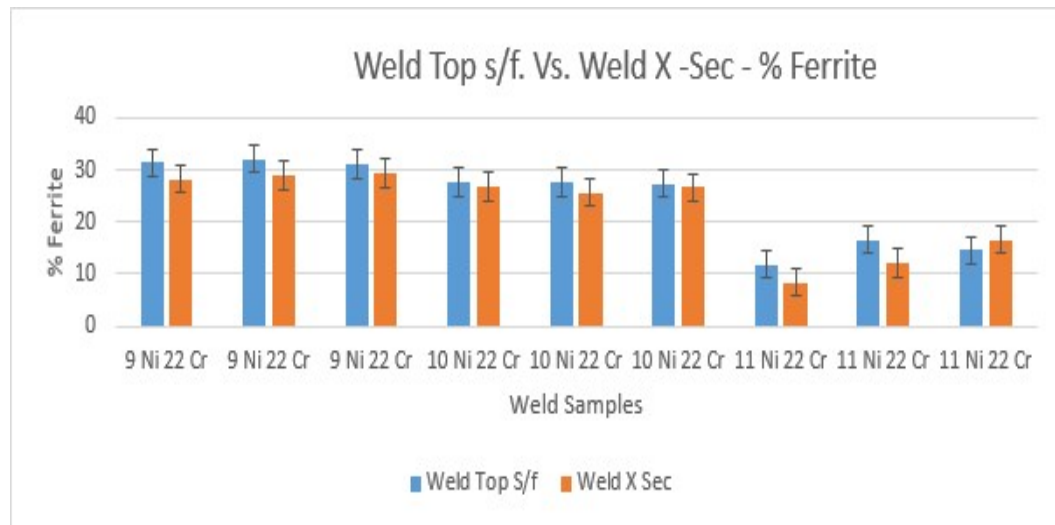


Fig. 5.20 Comparisons of ferrite measurement results between top surface of weld deposits and cross section of weld for different weld compositions considered under study.

Comparison of measured percentage ferrite and FN on all weld cross section by ASTM E 562, metallographic means and on weld centre line top surface by Feritscope® instrument show considerable variation with results obtained from Feritscope instrument, due to reason that in weld cross sections, the weld metal has been subjected to reheating by successive weld passes, results in some loss of ferrite. This fact can be revealed through scatter plots of Ferrite Number measurement data taken on centreline of weld deposit top surface and weld cross section for all weld compositions using Feritscope instrument only. As shown in Fig.5.21, 5.22,5.23 & 5.24.

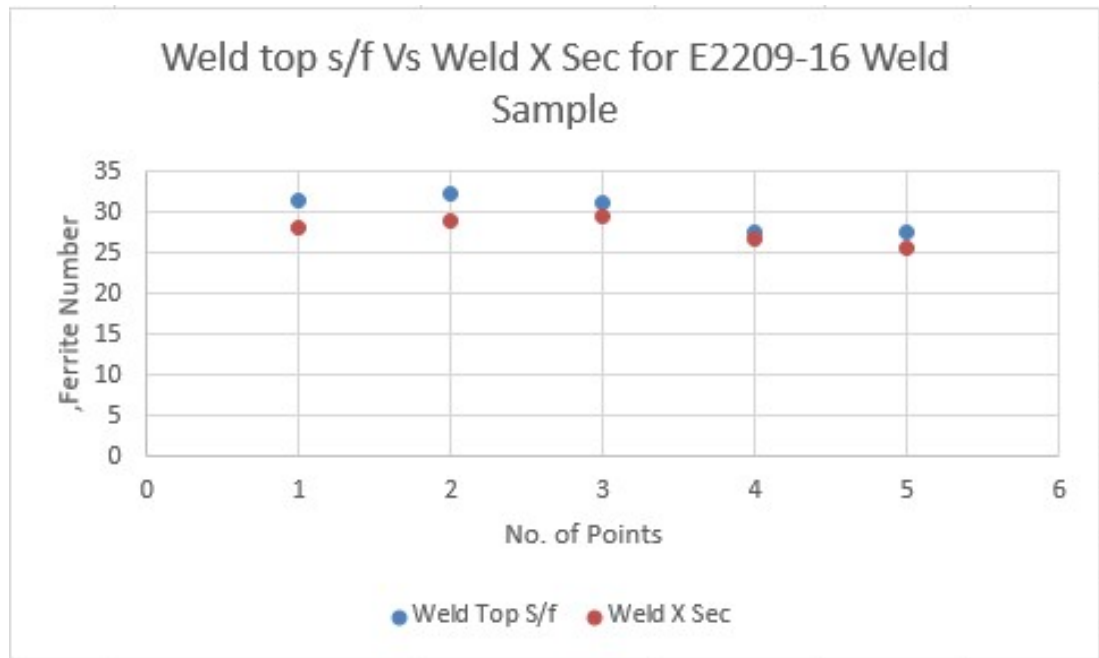


Fig. 5.21 Scatter plot of FN measurement on weld top surface centre line and on weld cross section for E2209-16 weld sample.

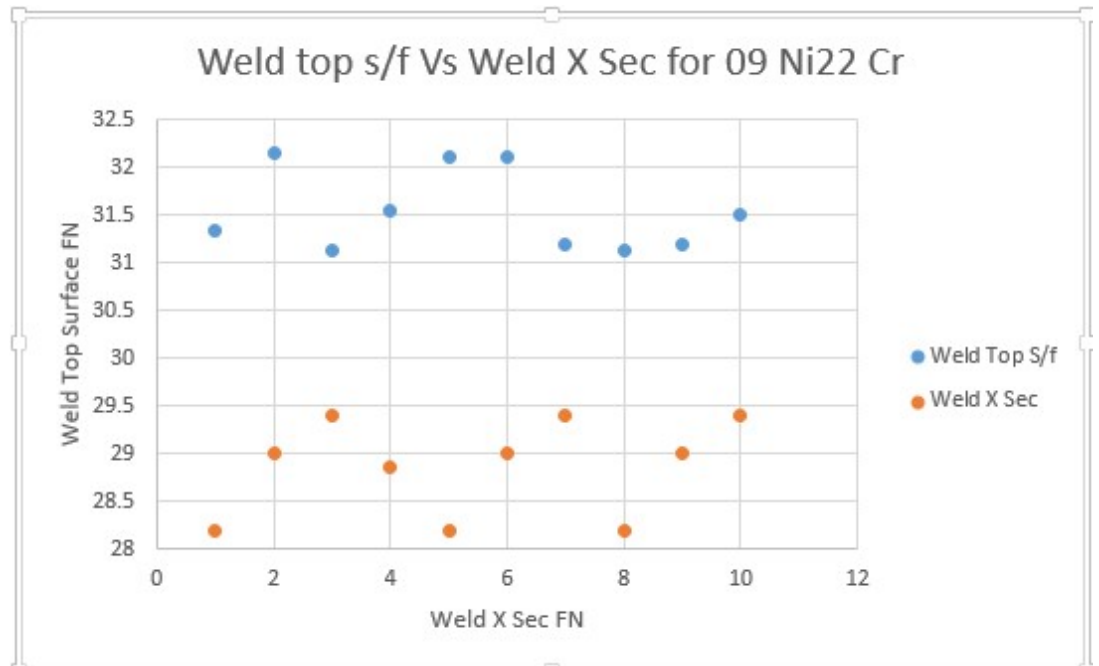


Fig. 5.22 Scatter plot of FN measurement on weld top surface centre line and on weld cross section for 9 Ni 22 Cr weld sample.

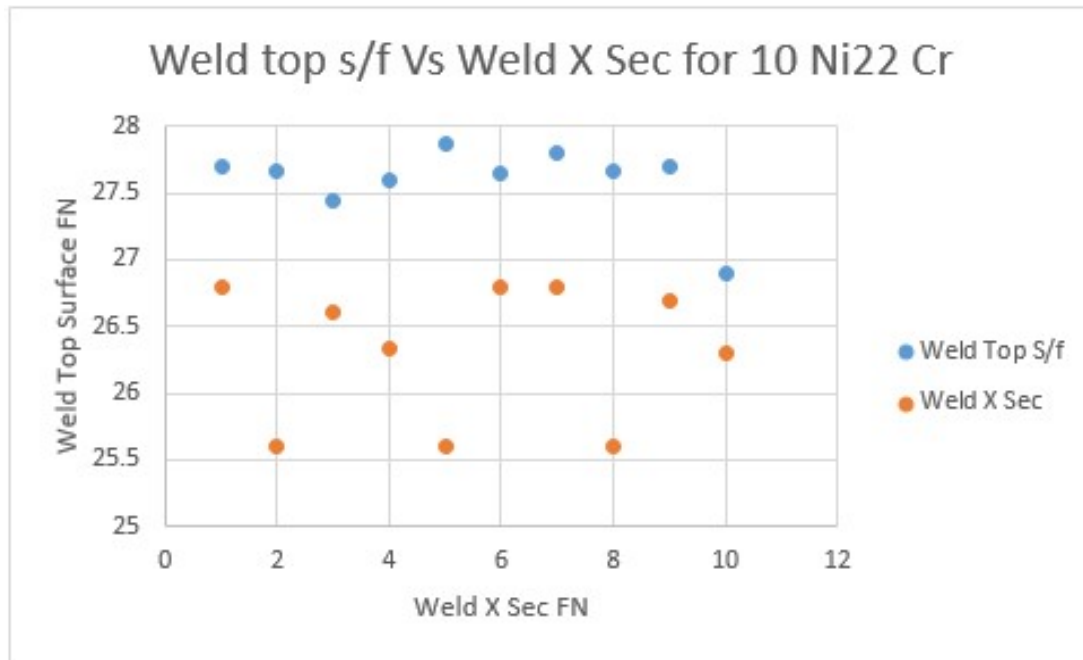


Fig. 5.23 Scatter plot of FN measurement on weld top surface centre line and on weld cross section for 10 Ni 22 Cr weld sample.

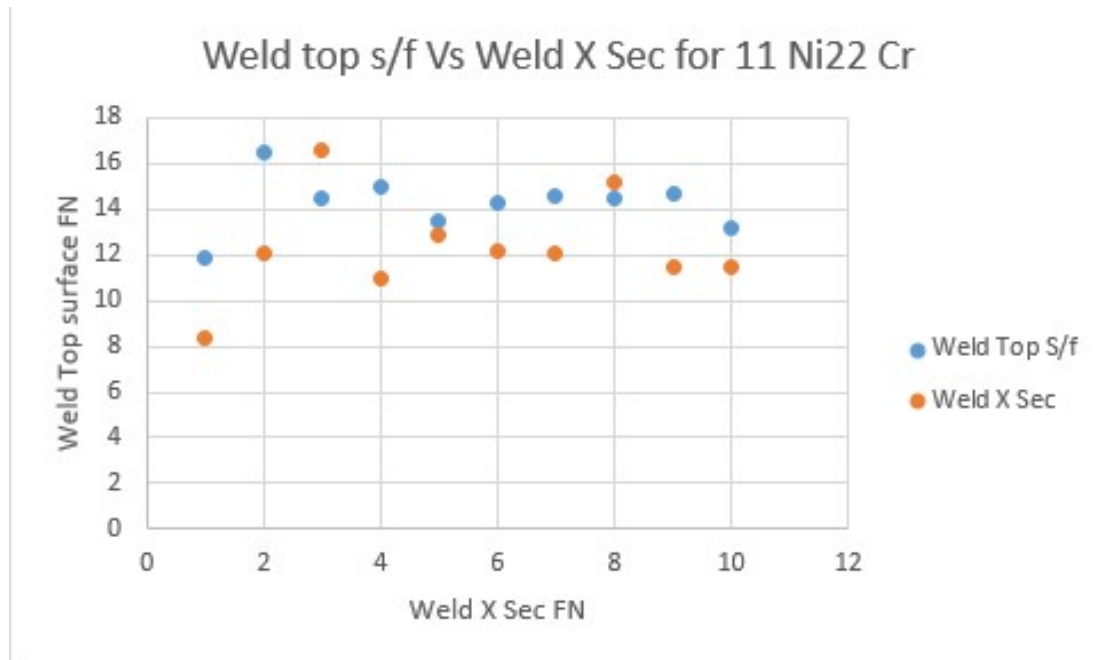


Fig. 5.24 Scatter plot of FN measurement on weld top surface centre line and on weld cross section for 11 Ni 22 Cr weld sample.

5.6 Comparisons of Ferrite Measurement results between WRC-1992 diagram (Predictive method) and Feritscope Instrument (Actual Measurement method)

Considering the 15-20% contributions from base metal faying surfaces and 60-70 % contributions from filler metals, under two situations of weld metal dilutions, WRC-1992 diagrams prepared for all weld compositions to be compared with the Feritscope® instrument methods. The scatter plots (WRC-1992 versus Ferritscope® method), as shown in Fig5.25. Shows that Feritscope results are more consistent, and exhibit linear tendencies, while values being less scattered from the mean value than those of the WRC 1992 (predictive) method. This difference is due to rapid weld thermal cyclic changes in weld metal dilutions occurring during actual welding process.

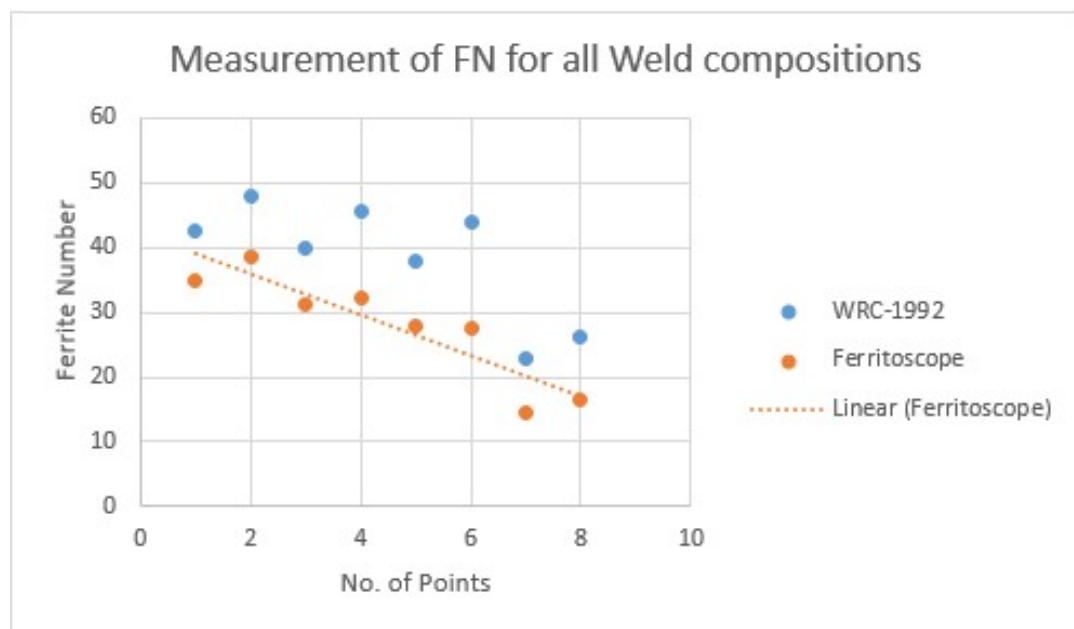


Fig. 5.25 Scatter Plot of FN measurement results comparing WRC-1992 (predicted value) and Ferritscope instrument (measured value) for all weld compositions (E2209-16, 9 Ni 22 Cr, 10 Ni 22 Cr and 11 Ni 22 Cr).

Table 5.2 FN measurement results of WRC-1992 (predicted value) and Feritscope Instrument (measured value) for all weld compositions

| Weld coupon ID | WRC-1992 | Feritscope |
|----------------|----------|------------|
| E2209-16 | 42.7 | 35 |
| E2209-16 | 48 | 38.5 |
| 9 Ni 22 Cr | 39.9 | 31.34 |
| 9 Ni 22 Cr | 45.5 | 32.16 |
| 10 Ni 22 Cr | 37.9 | 27.7 |
| 10 Ni 22 Cr | 44 | 27.66 |
| 11 Ni 22 Cr | 22.7 | 14.5 |
| 11 Ni 22 Cr | 26.3 | 16.52 |

5.7 Effect of ferrite content on pitting behaviour

Results of pitting corrosion as per ASTM G48 Method- A, indicates very marginal loss of weight ranging from 0.0003 to 0.0007 gms only. Whereas corrosion rate measured 0.15 to 0.32 in gm/m². Samples were observed at 20 X magnification. None of the sample exhibited pitting corrosion even after 24 hrs of exposure in 6 % FeCl₃ test solutions at 22 °C as shown in Table 5.3.

Table 5.3 ASTM G48A pitting test results

| Coupon Id | 10 Ni 22 Cr (Low Ni) | 11 Ni 22 Cr (Medium Ni) | 12 Ni 22 Cr (High Ni) |
|--|---|--|---|
| Sample Photo at 20 X magnification |  20 X Magnification |  20 X Magnification |  20 X Magnification |
| Weight Loss in gms | 0.0003 | 0.0007 | 0.0007 |
| Corrosion rate in gm/m ² | 0.15 | 0.36 | 0.32 |

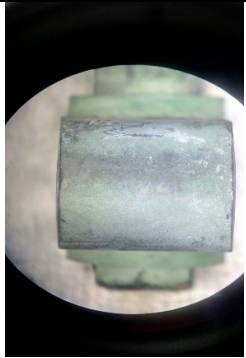
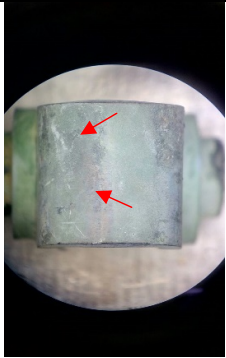
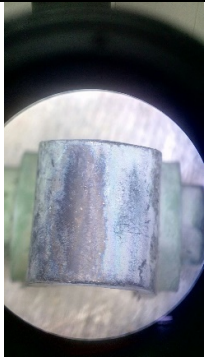
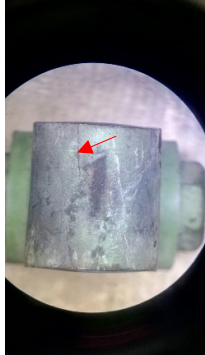
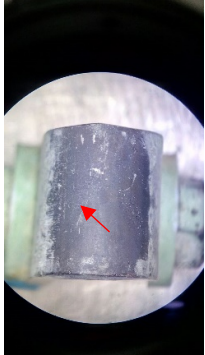
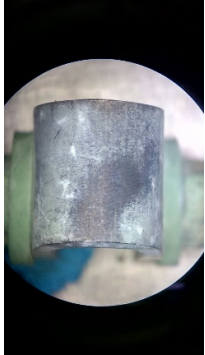
5.8 Effect of ferrite content on Stress Corrosion cracking susceptibility

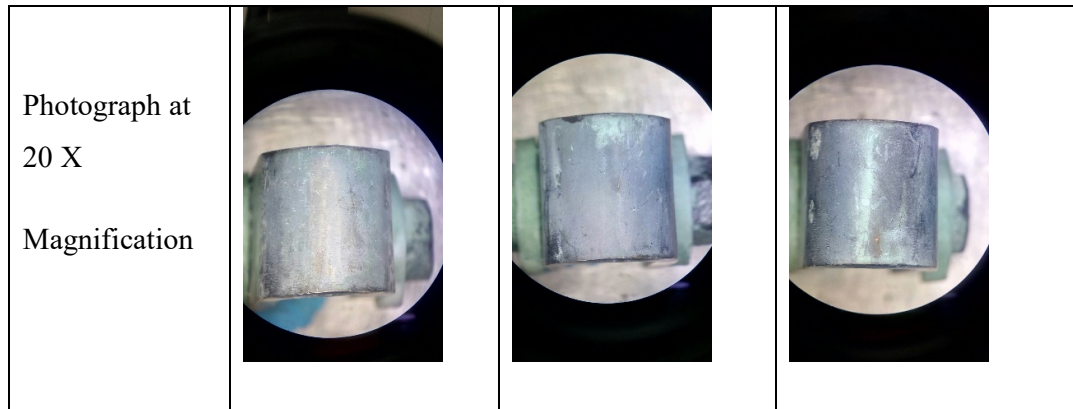
All weld metal test results clearly mentions that filler metal can satisfactorily meet all mechanical property requirements now we need only the chloride stress corrosion cracking test to determine if these filler metals meet corrosion requirements.

The specimen were periodically removed from flask after one week, for examining the specimen under 20 X magnification for the cracks and test solution pH. The solution changed at scheduled interval and this process has been repeated for scheduled time interval as after 6 h, daily for one week, and weekly for six weeks up to 1000 hrs (or 4-weeks), as per mentioned in ASTM G123 Standard.

Specimens were properly rinsed and dried, and examined under 20 X magnification for cracks appearance. The observations of specimen photograph at regular interval as shown in table 5.4 show that the weld sample prepared with 10% Ni filler metal exhibit cracks after 21 days (504 hours) but not after 1000 hours having ferrite % below 32 approximately. No SCC cracking was observed after 1000 hours exposure in any of the samples prepared with 12% nickel having ferrite below 15 %.

Table 5.4 Periodic observation of CSSC Samples at bend portion 20 X magnification

| Coupon ID | Observations | | |
|----------------------------------|---|--|---|
| | Sample A | Sample B | Sample C |
| 10 Ni 22 Cr Low Ni | No crack observed at bend portion at exposure of 1000 hrs. | Crack observed at bend portion after 3 weeks(21 days,504 hours) | No crack observed a bend portion at exposure of 1000 hrs. |
| Photograph at 20 X Magnification |  |  |  |
| 11 Ni 22 Cr Medium Ni | Crack observed at bend portion after 2 weeks (14 days,366 hours) | Crack observed at bend portion after 2 weeks(14 days,366 hours) | No crack observed at bend portion at exposure of 1000 hours. |
| Photograph at 20 X Magnification |  |  |  |
| 12 Ni 22 Cr High Ni | No crack observed at bend portion at exposure of 1000 hrs. | No crack observed at bend portion at exposure of 1000 hrs. | No crack observed at bend portion at exposure of 1000 hrs. |



All observations are made regularly as per schedule mentioned in the standard but above Table No. 5.4 includes only those photos of samples, which exhibited cracks at certain time interval and also photos of unaffected all weld samples up to the specified maximum duration of the test program (i.e. 1000 Hrs.)

Cross sections of the samples revealing cracks were taken (Fig 5.28 (C) & (d) on the outer diameter portion of 11 Ni 22 Cr sample A & B, which revealed cracks. The effort was to confirm if the crack developed is of “branched” or “network” type, which is a typical appearance of the SCC crack. So cross sectioned samples were polished carefully and etched using 10 % ammonium persulfate (electrolyte) as per ASTM E407-07 practice and were examined under optical microscope at 100 - 400 X magnification as shown in Fig 5.26 (a-b), 5.27 (a-b) & 5.28 (a-b). Higher magnification photomicrographs of the crack cross sections seem to clearly establish that the cracks are SCC.

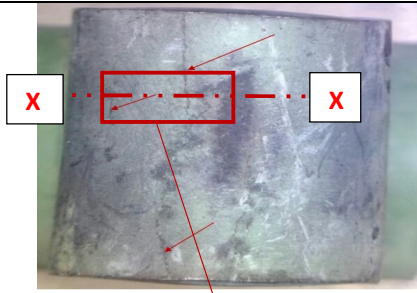


**Fig. 5.26 (a) 11 Ni 22Cr Coupon A
Crack after 2 weeks**

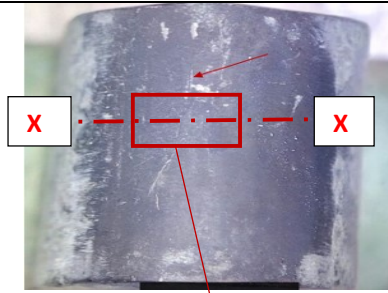


**Fig. 5.27 (a) 11Ni22Cr Coupon B
Crack after 2 weeks**

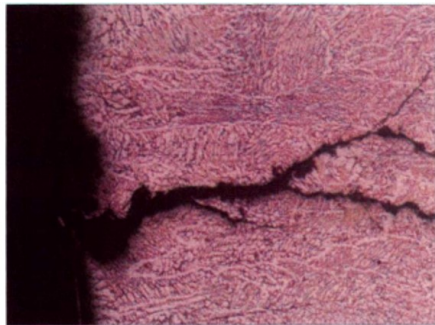


Plate 1: At Od 100 X

**Fig. 5.26 (b)
Crack cross section
photomicrograph at etched with 10
% Ammonium Persulfate
(Electrolyte) view at 100 X
magnification revealed typical SCC
Crack.**

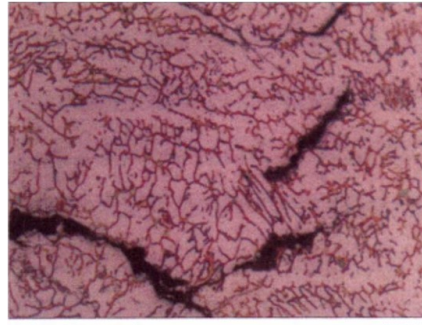


Plate 2: At od 400 X

**Fig. 5.27 (b)
Crack cross section
photomicrograph at etched with
10 % Ammonium Persulfate
(Electrolyte) view at 400 X
magnification revealed trans
granular typical SCC Crack**



**Fig 5.28 (c) & (d)
Perspective Views of
Cross sectioned SCC
specimen**